European Journal of Radiology Open 14 (2025) 100650

Contents lists available at ScienceDirect

European Journal of Radiology Open

journal homepage: www.elsevier.com/locate/ejro

Preoperative MR - based model for predicting prognosis in patients with intracranial extraventricular ependymoma

Liyan Li [a,1], Xueying Wang [b,1], Zeming Tan [c,1], Yipu Mao [d], Deyou Huang [e], Xiaoping Yi [b,f,g,h,i,j,*], Muliang Jiang [a,*], Bihong T. Chen [k]

[a] Department of Radiology, First Affiliated Hospital of Guangxi Medical University, Nanning, Guangxi 530021, PR China
[b] Department of Dermatology, Xiangya Hospital, Central South University, Changsha, Hunan 410008, PR China
[c] Department of Neurosurgery, Xiangya Hospital, Central South University, Changsha, Hunan 410008, PR China
[d] Department of Radiology, Nanning First People's Hospital, Nanning, Guangxi 530021, PR China
[e] Department of Radiology, Affiliated Hospital of Youjiang Medical University for Nationalities, Baise, Guangxi 533000, PR China
[f] National Engineering Research Center of Personalized Diagnostic and Therapeutic Technology, Xiangya Hospital, Changsha, Hunan 410008, PR China
[g] National Clinical Research Center for Geriatric Disorders (Xiangya Hospital), Central South University, Changsha, Hunan 410008, PR China
[h] Hunan Key Laboratory of Skin Cancer and Psoriasis, Xiangya Hospital, Central, South University, Changsha, Hunan 410008, PR China
[i] Hunan Engineering Research Center of Skin Health and Disease, Xiangya Hospital, Central South University, Changsha, Hunan 410008, PR China
[j] Department of Dermatology, Xiangya Hospital, Central South University, Changsha, Hunan 410008, PR China
[k] Department of Diagnostic Radiology, City of Hope National Medical Center, Duarte, CA, USA

HIGHLIGHTS

- Prognostic evaluation in patients with intracranial extraventricular ependymoma (IEE) could aid disease management.
- MR imaging features such as tumor location (F1), eloquent brain (F3), T1/FLAIR ratio (F10), and definition of the non-enhancing margin(F13) were associated with prognosis in patients with IEE.
- A nomogram based on clinical data and MRI-VASARI features could potentially be used for survival analysis in patients with IEE.

ARTICLE INFO

Keywords:
Intracranial extraventricular ependymoma
proportional hazards
survival analysis
VASARI (Visually AcceSAble Rembrandt Images) features
Magnetic resonance imaging

ABSTRACT

Objectives: To develop and validate a prediction model based on brain MRI features to predict disease-free survival (DFS) and overall survival (OS) for patients with intracranial extraventricular ependymoma (IEE).
Methods: The study included 114 patients with pathology-proven IEE, of whom 80 were randomly assigned to a training group and 34 to a validation group. Preoperative brain MRI images were assessed with the Visually AcceSAble Rembrandt Images (VASARI) feature set. Clinical variables were assessed including age, gender, KPS, pathological grade of the tumor and blood test data such as eosinophil, blood urea nitrogen and serum creatinine. Multivariate Cox proportional hazards regression analysis was performed to select the independent prognostic factors for DFS and OS. Three prediction models were built with clinical variables, MRI-VASARI features, and combined clinical and MRI-VASARI data, respectively. The predictive power of survival models was assessed using c-index and calibration curve.
Results: Clinical variables such as eosinophil, blood urea nitrogen and serum creatinine, and MRI-VASARI feature for definition of the non-enhancing margin (F13) were significantly correlated with the prognosis of DFS. Blood urea nitrogen, D-dimer, tumor location (F1), eloquent brain (F3), and T1/FLAIR ratio (F10) were independent

Abbreviations: **BUN**, Blood urea nitrogen; **C-index,**, Concordance index; **CI,**, Confidence interval; **DFS,**, Disease-free survival; **Eos,**, Eosinophil; **GBM,**, Glioblastoma multiforme; **HR,**, Hazard ratio; **IEE,**, Intracranial extraventricular ependymoma; **KM,**, Kaplan-Meier survival curve; **KPS,**, Karnofsky performance status; **MRI,**, Magnetic resonance imaging; **OS,**, Overall survival; **Scr,**, Serum creatinine; **TCGA,**, The cancer genome atlas; **TCIA,**, The cancer imaging archive; **VASARI,**, Visually AcceSAble Rembrandt Images.

* Correspondence to: Department of Radiology, Xiangya Hospital, Central South University, No. 87 Xiangya Road, PR China.
* Corresponding author.
E-mail addresses: yixiaoping@csu.edu.cn (X. Yi), jmlgxmu@gmail.com (M. Jiang).
[1] These authors contributed equally.

https://doi.org/10.1016/j.ejro.2025.100650
Received 4 February 2025; Received in revised form 19 March 2025; Accepted 31 March 2025

predictors of OS. Based on these factors, prediction models were constructed. The concordance indices of the three survival models for OS were 0.732, 0.729, and 0.768, respectively. For DFS, the concordance indices were respectively 0.694, 0.576, and 0.714.
Conclusion: Predictive modelling combining both clinical and MRI-VASARI features is robust and may assist in the assessment of prognosis in patients with IEE.

1. Introduction

Ependymomas are rare neuroepithelial tumors, accounting for only 6.9 % of primary central nervous system tumors diagnosed annually [1]. Although the majority of ependymomas originate as a neoplastic transformation of cells in the ventricular system, it could occur anywhere and could be located outside the ventricles as the intracranial extraventricular ependymoma (IEE)[2,3]. Ependymomas have been categorized into supratentorial, posterior cranial fossa, spinal cord, mucinous papillary ependymomas, and subependymomas based on a combination of histological and molecular characteristics, according to the World Health Organization's classification of central nervous system tumors in 2021[4,5]. However, the histological classification of ependymomas is not applicable to the 2021 update of the WHO Central Nervous System Tumor Classification, which also introduces genotyping [3]. For example, supratentorial ependymoma with ZFTA fusion (ST-ZFTA) mainly occurs near the ventricular system, but may also occur outside the ventricle and in the cortex[3]. About 50 % of patients with ependymomas will recur, with a median time to recurrence of 13–25 months[6–8]. In pediatric patients, the 10-year overall survival (OS) at 50–73 % [9] and disease-free survival (DFS) at 3–7 years being 30–61 % have been reported[8,10,11]. In adults with ependymoma, 5-year DFS and OS have been reported to be around 40 %–50 % and 60 %–70 %, respectively[8,12]. Prognostic assessment for patients with IEE may assist in treatment planning.

Prognostic factors for ependymoma such as the age, tumor location, high Karnofsky performance status (KPS), and extent of surgical resection have been reported [10,13–15]. However, literature is inconclusive. For instance, a prior study showed factors such as age, patient sex and postoperative radiation not being prognostic for survival [16]. More studies are needed to assess the predictors for survival. Nomogram has been used to predict tumor prognosis by scoring risk factors [17] and to predict survival in various cancer such as hepatocellular, laryngeal, pancreatic, and esophageal cancers [18–21]. It is prudent to develop non-invasive models and nomograms for prognostic assessment.

Magnetic resonance imaging (MRI) has been routinely acquired for patients with IEE. The Visually AcceSAble Rembrandt Image (VASARI) MRI-based feature has been developed for the standardized analysis of MRI features of brain tumors. The VASARI feature set has been used for prediction of survival [22–24] and tumor progression [25]. Rao et al. analyzed the TCGA (The Cancer Genome Atlas) glioblastoma multiforme dataset, and identified relevant VASARI features such as tumor volume, T1/FLAIR ratio, and tumor hemorrhage as prognostic predictors for survival [26]. However, literature is limited on the VASARI features and imaging predictors for prognosis of IEE. Prediction models are developed and validated by combining the predictors statistically into a multivariable model. The Cox regression model is one of the prediction models that has been commonly used in clinical research by assuming some linear relationship between a given covariate (such as age) and the research results [27]. A prior study by Sun et al. combined 14 prognostic and clinical factors and constructed a Cox regression model for lung adenocarcinoma, which showed good predictive performance [28]. Developing prediction models with Cox regression, machine learning and or artificial intelligence approach should aid in clinical decision making such as risk-stratification for treatment selection and clinical trial participation for patients with brain tumors [29]. However, literature is limited in predictive modeling with clinical variables and MRI-VSARI for survival prediction in patients with IEE.

In this retrospective multi-center study, we identified a cohort of patients with pathologically confirmed IEE. The predictive power of the clinical variables and the MRI-VASARI features for DFS and OS in patients with IEE was assessed and a Cox proportional hazards regression model incorporating MRI-VASARI features and clinical variables were built for predicting survival for patients with IEE. The results of this study should help to advance our knowledge about this rare brain tumor and assist in its clinical management.

2. Materials and methods

2.1. Patients

This study was approved by the ethics committees of all participating hospitals and the informed consent was not required because of the retrospective nature of this study.

A total of 114 patients with IEE confirmed by surgical pathology between June 2016 and June 2021 were included from the participating hospitals. These patients were divided into training (80 patients) and validation (34 patients) groups at random in a 7:3 ratio. Details of the exclusion criteria and the reasons for exclusion are presented in Fig. 1. There was partial cohort sharing with our own previous publication[30] but for a different purpose. The previous study was focused on distinguishing IEE from glioblastoma multiforme using neuroimaging features, while the present study was focused on predicting survival in patients with IEE using MRI-based prediction models. Besides, the present study only assessed IEE features, without involving any comparative analysis with GBM as the previous study. The present study should be considered as a continuation and extension of the previous study because it contributed new information on survival prediction and was complimentary to the study results from the previous study about brain tumors.

The clinical variables and brain MRI-VASARI features of the patients were recorded. The assessed clinical variables included age, gender, KPS, and pathological grade of the tumor and laboratory blood test data such as eosinophil, blood urea nitrogen and serum creatinine values. The OS was defined from the end of surgical resection to the time of death (death was reported in 23 patients). DFS was calculated as the time from the end of surgical resection to disease recurrence or death due to disease progression (52 patients reported recurrence or death). This study was performed in accordance with the Transparent Reporting of a multivariable prediction model for Individual Prognosis or Diagnosis (TRIPOD) reporting checklist[29], which was included in our previous study of IEE for a different purpose[30].

2.2. Preoperative MRI image acquisition

Brain MRI images were obtained in a 3 Telsa GE scanner (GE Medical Systems Discovery MR750w), a 1.5 Telsa Siemens scanner (Siemens Medical Systems MAGNETOM Avanto or Sempra), or a 3 Telsa Siemens scanner (Siemens Medical Systems Magnetom Verio). Routine standardized brain MRI scanning was performed, including T1-weighted images (T1WI), T1-weighted with gadolinium contrast-agent (T1WI+C), T2-weighted (T2WI), and T2-weighted with fluid-attenuated inversion recovery (T2-FLAIR). All sequences were acquired at the FOV of 220 × 220 mm, slice thickness of 5 mm, matrix of 256 × 256, and slice spacing (1 mm), as indicated in previous studies [31–33].

The MRI images were independently reviewed by 2 neuroradiologists (X.L and Y.Q, with 15 and 20 years of experience, respectively) who were not aware of the clinicopathological data. Imaging results were recorded by consensus. For the cases that did not reach consensus, a third experienced neuroradiologist (L.L, with more than 30 years of experience) would make the final decision.

2.3. MRI-VASARI imaging features

All brain MRI images for the cohort were assessed using the VASARI feature set. Each lesion was scored as previously described, with 30 imaging features being evaluated (F1-F30) [33,34]. Among these 30 features, 27 were ultimately used, while three features such as F26, F27, and F28 were excluded due to lack of post-surgical MRI images in some patients.

2.4. Statistical analysis and model construction

This cohort was randomly divided into a training group and a validation group. A univariate Cox proportional hazards regression analysis was used for selecting the most robust survival-related features. Subsequently, a multivariate Cox proportional hazards regression analysis was performed to determine the independent prognostic factors for survival with features obtained from univariate analysis with a p-value < 0.05. A survival prediction model was constructed based on the independent prognostic factors for the training group and was visualized on a nomogram plot. Three prediction models were built with clinical variables, MRI-VASARI features, and combined clinical and MRI-VASARI data, respectively. The predictive power of survival models was assessed using concordance index (c-index) and calibration curve.

Cox proportional hazards regression models estimated a hazard ratio (HR) and corresponding 95 % confidence interval (CI) for each potential risk factor. The 3-year, 5- year, and 7-year survival rates were the endpoints of the nomogram. The nomogram-predicted survival probability was compared with the observed survival probability, calculated with the Kaplan–Meier method in the training group and the validation group. The validation of the nomogram was performed using the c-index and the calibration curve. The c-index was used to estimate the predictive accuracy and discriminating ability of each model and the overall nomogram: the higher the c-index, the better its prognostic accuracy. The "survival" R package was used to evaluate the consistency of the nomogram and to make the calibration curves. The agreement between the observed 3-, 5-, and 7-year survival rates and the nomogram-predicted survival rates was evaluated using the calibration curves. The "survdiff" package from R was used for the log-rank test and $p < 0.05$ was considered to be statistically significant. Log-rank tests with the linear trend for factor levels were performed to test for significant associations between those features and DFS or OS.

3. Results

A total of 114 patients (78 male and 36 female patients) with IEE were included in this study (median age:22.0 years, IQR: 10–44 years). There were 80 and 34 patients, respectively, drawn at random for the training and validation groups. There were no significant differences in the clinicopathologic characteristics between the training and the validation groups (all p values >0.05) (Table 1). The range for DFS was 1.00–178.70 months and the median time was 30.10 months. The range for OS was 3.40–183.20 months and the median time was 35.65 months. Fig. 1 presents the diagram for study flow.

Table 1
Demographic, clinical and MRI-VASARI (Visually Accessible Rembrandt Images) features of patients with intracranial extraventricular ependymoma (IEE).

Characteristic	Training group (n = 80)	Validation group (n = 34)	*P*-value
Demographics characteristics			
Gender, n (%)			0.38
Male	57(71.25 %)	21(61.76 %)	
Female	23(28.75 %)	13(38.24 %)	
Age [median (IQR), years]	23.50 (12.00–47.75)	13.00 (5.00–37.75)	0.06
Clinical characteristics [mean , (SD)]			
Eos	0.16 (0.19)	0.23 (0.36)	0.25
BUN	3.68 (1.87)	3.63 (1.58)	0.93
Scr	65.00 (23.12)	60.81 (35.65)	0.07
D-dimer	0.31(0.65)	0.34(0.55)	0.83
DFS, n (%)			0.55
0	42 (52.50 %)	20 (58.82 %)	
1	38 (47.50 %)	14 (41.18 %)	
OS, n (%)			0.13
0	67 (83.75 %)	24 (70.59 %)	
1	13 (16.25 %)	10 (29.41 %)	
VASARI features [mean, (SD)]			
F1	3.05 (2.52)	3.00 (2.46)	0.63
F3	1.61 (1.14)	1.79 (1.27)	0.98
F10	1.58 (0.55)	1.68 (0.59)	0.62
F13	2.71 (0.48)	2.65 (0.65)	0.10

Significant at $P < 0.05$.
Note: F1, tumor locations; F3, eloquent brain; F10, T1/FLAIR ratio; F13, definition of the non-enhancing margin. For disease-free survival (DFS) and overall survival (OS), 0 represents that no endpoint event has occurred, while 1 represents that an endpoint event has occurred.
Abbreviations: Eos, Eosinophil; BUN, blood urea nitrogen; Scr, Serum creatinine.

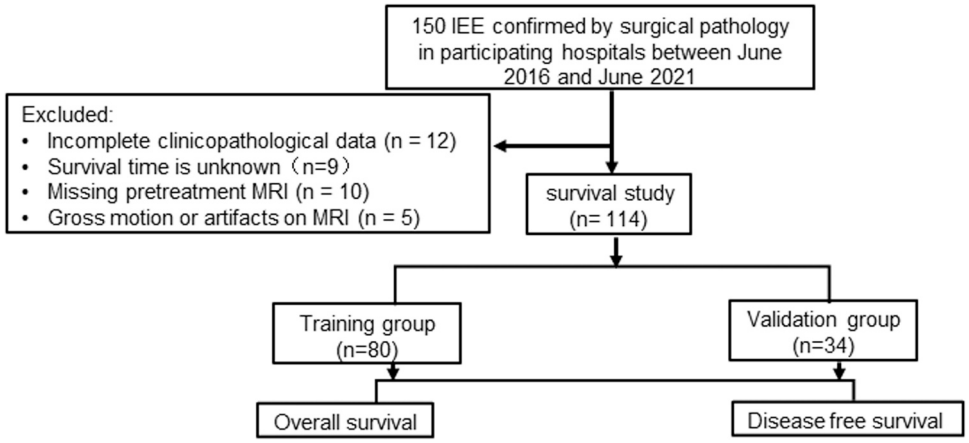

Fig. 1. Flowchart for enrolling the study cohort of patients with intracranial extraventricular ependymoma (IEE).

In the training group, multivariate Cox proportional hazards regression analysis identified the clinical variables such as eosinophil, blood urea nitrogen, serum creatine, and MRI-VASARI feature such as F13 as significant prognostic factors for DFS (Table 2). The factors including blood urea nitrogen, D-dimer, F1, F3, and F10 were significant predictors for OS ($p < 0.05$) (Table 3).

We constructed three prediction models based on clinical data, MRI-VASARI feature, and the clinical and imaging feature combined, respectively (Table 4). For OS, the clinical prediction model had a c-index of 0.732, the MRI-VASARI feature-based model had a c-index of 0.729, and model combining both clinical and MRI-VASARI features had a c-index test of 0.768. For DFS, the c-indices for clinical, MRI-VASARI and combined models were 0.694, 0.576, and 0.714, respectively. The results showed that the c-index of the combined model incorporating both clinical and MRI-VASARI features was the highest among the three models.

Fig. 2 presents the predicted probabilities and visualized nomograms for 3-, 5-, and 7-year survival in patients with IEE. The model incorporated all factors related to survival. The nomogram plot revealed that blood urea nitrogen and eosinophil had the strongest correlations with OS and DFS, respectively. D-dimer, serum creatinine, F1, F3, F10, and F13 were the next most significant predictors of survival. Each variable was assigned a score according to its prognostic value. The total score for all variables was converted into predictions of 3-, 5-, and 7-year survival probabilities for OS and DFS. The scores for each chosen variable could be used to calculate the likelihood that the patient would survive. Calibration curves were used to graphically evaluate the nomograms and found good agreement in predicting 3-, 5-, and 7-year survival in the training and validation groups (Fig. 3).

Kaplan-Meier survival curves calculated the endpoints of each event on different models separately and produced a relevant separation of OS and DFS survival curves (Fig. 4). Log-rank tests were performed for DFS and OS. Only the combined model had a p-value closest to 0.05 for DFS. For OS, both the MRI-VASARI features model and the combined model had a p-value < 0.05. The smaller the p-value of the log-rank test showed the more significant difference existed in the survival distribution of the model.

4. Discussion

In this study, we found preoperative MRI-VASARI features including F1 (brain tumor location), F3 (eloquent brain), F10 (T1/ FLAIR ratio), and F13 (definition of the non-enhancing margin) being significant prognostic factors for survival. The combined model incorporating clinical variables such as blood test values and MRI-VASARI features yielded a reasonable performance for prediction of DFS and OS in patients with IEE. Our study presented the potential imaging-focused approach for predicting prognosis in patients with IEE.

Table 2
Multivariate Cox proportional hazards regression analysis of clinical and MRI-VASARI features for disease-free survival in patients with intracranial extraventricular ependymoma.

Variable	Hazard Ratio [95 % CI]	*P*-value
Clinic		
Eos	11.62 [1.94,69.66]	0.007
BUN	0.76 [0.57,1.02]	0.068
Scr	0.99 [0.97,1.01]	0.182
VASARI		
F13	0.56 [0.33,0.95]	0.030

Significant at $P < 0.05$.
Note: Data are hazard ratio estimates; 95 % confidence interval (CI) in parentheses for variables included in Cox regression models.
Abbreviations: Eos, Eosinophil; BUN, blood urea nitrogen; Scr, Serum creatinine; VASARI, Visually Accessible Rembrandt Images; F13 , definition of the non-enhancing margin.

Table 3
Multivariate Cox proportional hazards regression analysis of clinical and MRI-VASARI features for overall survival in patients with intracranial extraventricular ependymoma.

Clinic	Hazard Ratio [95 % CI]	*P*-value
BUN	0.60 [0.36,0.99]	0.046
D-dimer	1.60 [1.12,2.30]	0.010
VASARI		
F1	1.45 [1.13,1.86]	0.004
F3	1.41 [1.00,1.99]	0.049
F10	5.61 [1.79,17.61]	0.003

Significant at $P < 0.05$.
Note: Data are hazard ratio estimates; 95 % confidence interval (CI) in parentheses for variables included in Cox regression models.
Abbreviations: BUN, blood urea nitrogen; VASARI, Visually Accessible Rembrandt Images; F1, tumor locations; F3, eloquent brain; F10, T1/FLAIR ratio.

Table 4
Concordance index (C-index) for clinical, MRI-VASARI, and combined prognostic models.

	DFS		OS	
	Training (95 %CI)	**Validation (95 %CI)**	**Training (95 %CI)**	**Validation (95 %CI)**
Clinic	0.694 [0.596,0.791]	0.679 [0.548,0.810]	0.734 [0.559,0.908]	0.732 [0.592,0.872]
MRI-VASARI	0.576 [0.494,0.658]	0.596 [0.452,0.740]	0.821 [0.719,0.924]	0.729 [0.602,0.857]
Combined	0.714 [0.621,0.806]	0.683 [0.546,0.819]	0.848 [0.770,0.926]	0.768 [0.663,0.873]

Note: The 95 % confidence interval is indicated in parentheses. OS, overall survival, DFS, disease-free survival; VASARI, Visually Accessible Rembrandt Images.

Our finding regarding the robust performance of the combined model in predicting survival was consistent with the prior reports [22,35,36]. Prior studies found that a combined model with both clinical and imaging features had higher predictive power than the model using only preoperative clinical predictors in a study of older patients with glioblastoma [22,35]. Similar research findings were also noted in a study of patients with glioblastoma by Mazurski et al., who constructed a combined multivariate model based on MRI-VASARI imaging and clinical features [36]. A controlled lexicon in the MRI-VASARI feature set could improve inter-reader agreement and clinical management [36]. In addition, the MRI-VASARI features could be used as biomarkers to predict overall survival and improve model predictive ability in older patients with glioblastoma [35]. Our study contributed new information on the performance of the combined model in brain tumors other than glioblastoma.

We found MRI-VASARI features such as F1 (brain tumor location), F3 (eloquent brain), and F10 (T1/ FLAIR ratio) were associated with poor OS in patients with. The higher the F1 value indicated it being the more likely it was to involve infratentorial areas, such as the cerebellar hemisphere and the fourth ventricle. This was because tumor encasement of the cranial nerves and brainstem vasculature in posterior fossa might limit extent of tumor resection [4,37]. Safe maximal surgical resection has long been considered the best treatment for ependymoma. Gross total resection and tumor location were independent predictors of survival in patients with ependymoma [4]. Therefore, incomplete resection has an increased risk of tumor recurrence and cerebrospinal fluid (CSF) dissemination [4]. Our study found that eloquent brain (F3) invasion was a risk factor, which should not be surprising. Tumor in the visual cortex may have poor prognosis because complete surgical resection would not be possible [23]. We also found a high value of the T1/FLAIR ratio predicting a worse prognosis, which is consistent with the findings of NicolasJilwan et al., who found that a higher T1/FLAIR ratio implicated a more infiltrative tumor with aggressive tumor

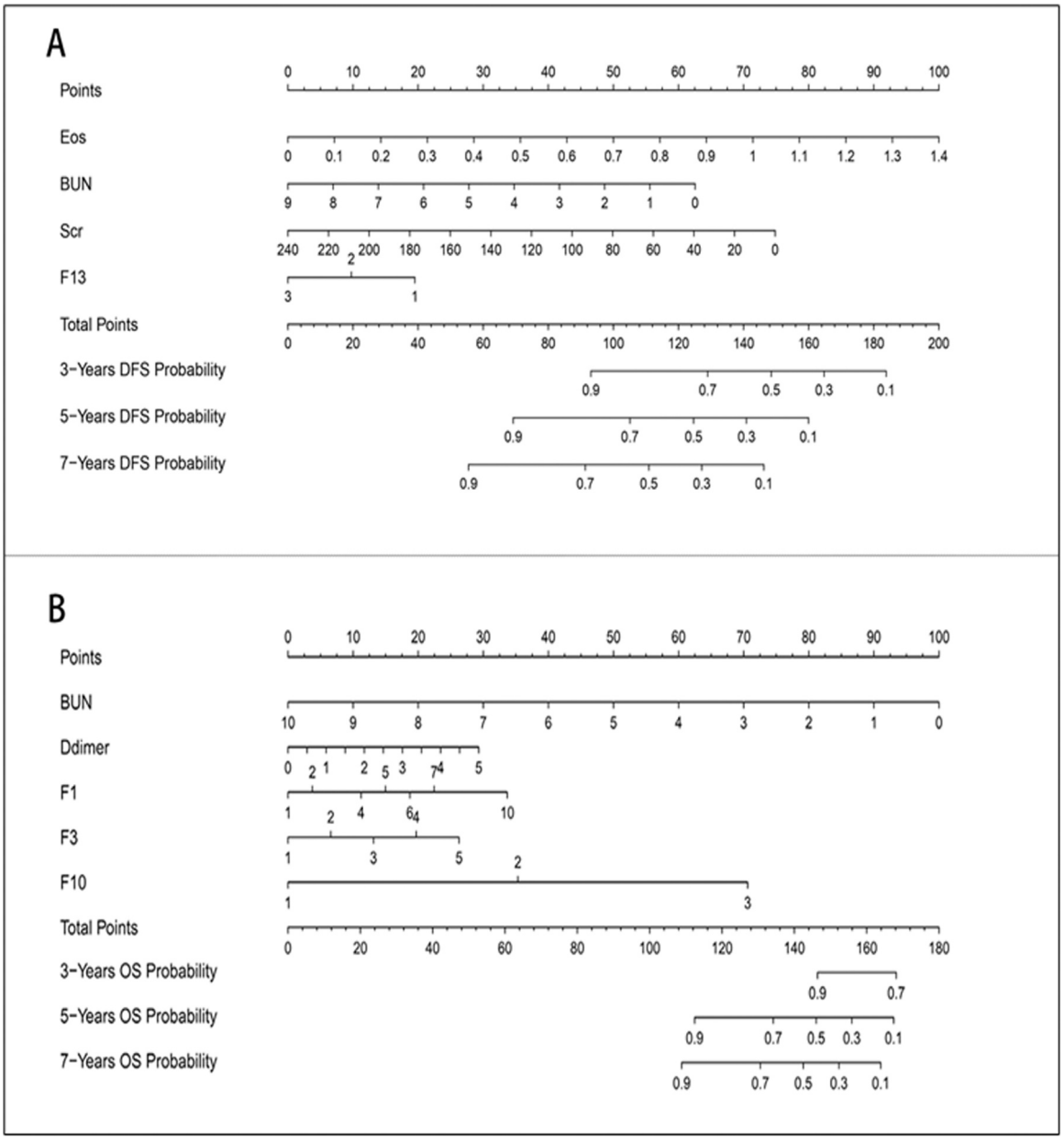

Fig. 2. Nomogram predicting 3-, 5- and 7- year disease-free survival (DFS) and overall survival (OS) of patients with intracranial extraventricular ependymoma (IEE). Note: The nomogram summed the points identified on the scale for each variable. The total points projected on the bottom scales indicate the probabilities of DFS and OS at 3-, 5-, and 7 years. A: nomogram for DFS; B: nomogram for OS. Abbreviations: Eos, Eosinophil; BUN, blood urea nitrogen; Scr, Serum creatinine; F1, tumor locations; F3, eloquent brain; F10, T1/FLAIR ratio; F13, definition of the non-enhancing margin.

behavior[23].

We observed the MRI-VASARI feature such as the definition of the non-enhancing margin (F13) being a protective factor in patients with IEE. In other words, patients with irregular, and non-enhancing tumor margins had a longer DFS than the patients with smooth non-enhancing margins in our study. This was inconsistent with a study by Zhou et al., which found smooth non-enhancing margins being associated with a longer survival compared with irregular non-enhancing margins in glioblastoma survival prediction [38]. We speculate that more extensive surgical resection may have been performed on the IEE with irregular tumor margins, thus reducing the probability of tumor recurrence and CSF dissemination and having better prognosis.

There were several limitations in this study. First, it was a retrospective study with small sample size covering a long-time span. Pathological specimen for some cases were no longer available and we could not perform additional molecular testing. Second, only internal validation was performed. We could not perform an independent external validation due to lack of an additional dataset, which may limit the generalizability of the prediction models. Third, there might be selection bias given its retrospective nature and patients with incomplete data excluded during data screening. In addition, there was a partial cohort sharing with our own previous publication [30], which may have introduced selection bias as study assessment was performed on the same IEE cohort that was already selected for the previous study. We believe the impact of the overlapping cohort to the present study results was minimal since the present study was carried out for survival prediction with no involvement of the other cohort, i.e., the glioblastoma multiforme group in the previous study. Lastly, because postoperative MR images and treatment data were not collected as part of the study, we did not have the follow-up data to test the model performance in patients after surgery. Therefore, further research including both pretreatment and postsurgical assessment is needed to verify the accuracy

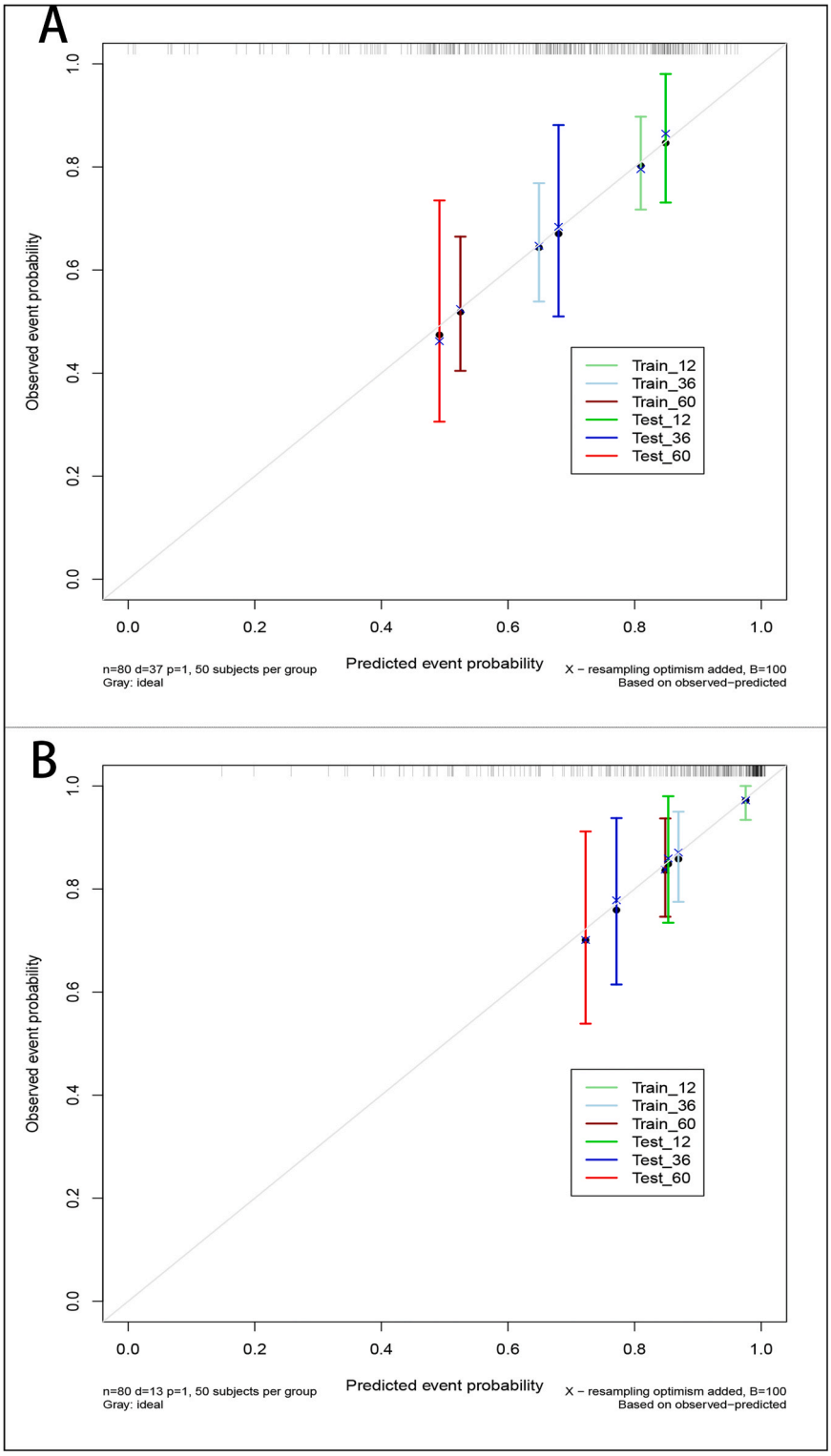

Fig. 3. Calibration curves for disease-free survival (DFS) and overall survival (OS) based on predictions of the nomogram. Note: Calibration curves for predicting (A) DFS and (B) OS in the training and validation cohorts. Nomogram predicted survival is plotted on the x-axis and actual survival is plotted on the y-axis.

of our prognostic model.

5. Conclusion

In summary, we developed a model for predicting prognosis of patients with IEE based on preoperative brain MR features and clinical variables. Future, prospective multicenter study with a larger sample size should be performed to validate our study result and to optimize the clinical application of the prediction model.

Ethics approval and consent to participate

The present study was approved by the Ethics Committee of all participating hospital including the First Affiliated Hospital of Guangxi

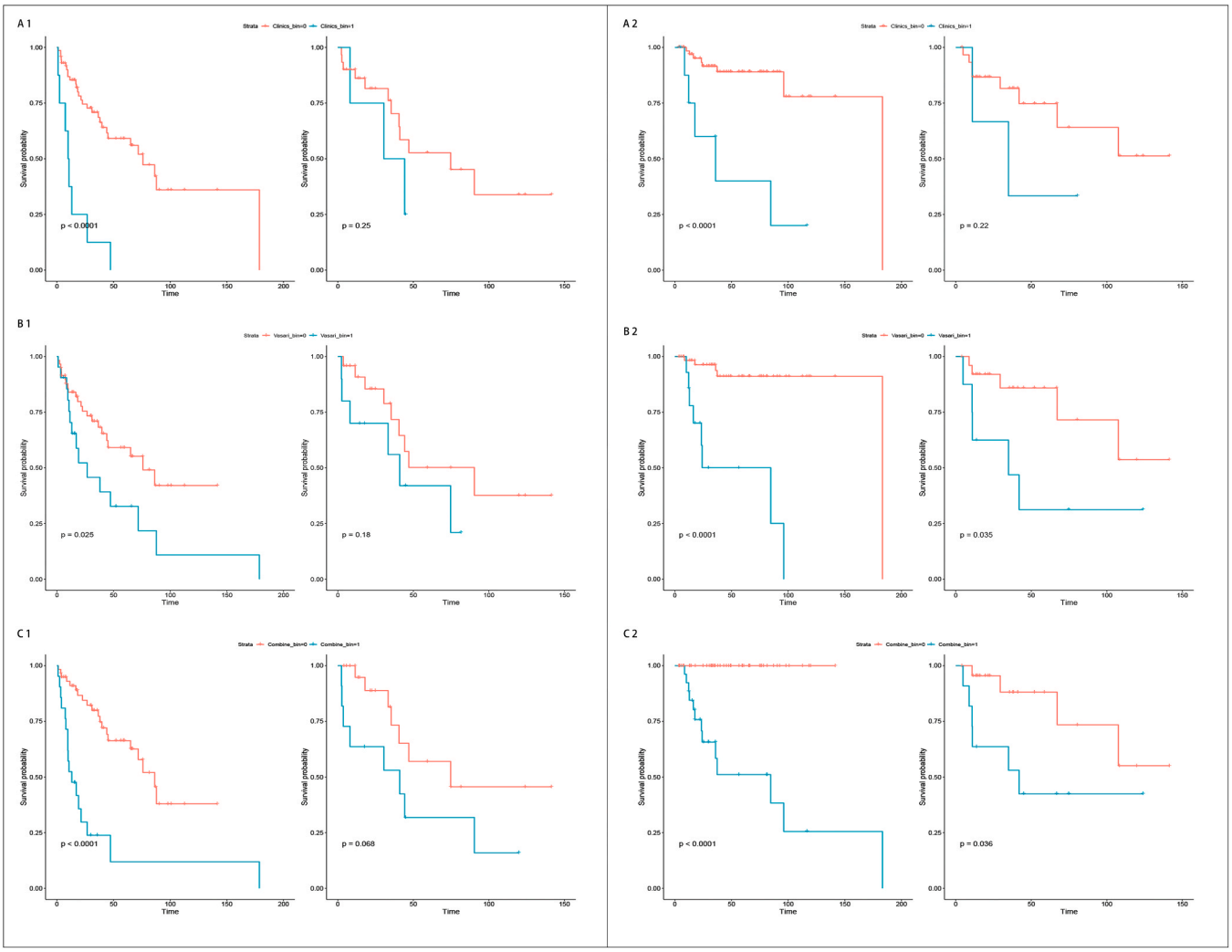

Fig. 4. Kaplan-Meier survival models for disease-free survival (DFS) and overall survival (OS). Note: A: Clinical model, B: MRI-VASARI model, and C: Combined model (1: disease-free survival (DFS), 2: overall survival (OS)). Each graph contained the training group on the left and the validation group on the right. The red line indicated the patients without an endpoint event (0), and the blue line indicated the patients with an endpoint event (1). The log-rank test was applied to test for significant separation of survival curves and calculation of *p*-values. Significant separation of DFS curves was observed in the combined model (C1) in the validation group ($p = 0.068$). Significant separation of the survival curves for OS was observed in the MRI-VASARI (B2) and combined (C2) models in the validation group ($p = 0.035$, $p = 0.036$).

Medical University (IRB#:2022-KY-E-(236)), Nanning First People's Hospital (IRB#:2022–196–01), and Xiangya Hospital, Central South University (IRB#: 202303034), P.R. China. Informed consent was waived due to the retrospective nature of this study.

Ethics approval and consent to participate

The present study was approved by the Ethics Committee of the First Affiliated Hospital of Guangxi Medical University (IRB#:2022-KY-E-(236)), Nanning First People's Hospital (IRB#:2022–196–01), and Xiangya Hospital, Central South University (IRB#: 202303034), P.R. China. Informed consent was waived due to the retrospective nature of this study.

Funding

This study was funded by National Science Foundation of China (Grant No. 82260344), Clinical Research "Climbing" Program from the First Affiliated Hospital of Guangxi Medical University (Grant No. YYZS2020021), Medical Excellence Award from the Creative Research Development Grant at the First Affiliated Hospital of Guangxi Medical University, P. R. China, the Project Program of National Clinical Research Center for Geriatric Disorders (Xiangya Hospital, Grant No. 2022LNJJ09).

CRediT authorship contribution statement

Tan Zeming: Formal analysis, Data curation. **Wang Xueying:** Data curation. **Li Liyan:** Writing – original draft, Data curation. **Chen Bihong T. T.:** Writing – review & editing. **Jiang Muliang:** Writing – review & editing, Methodology, Funding acquisition, Data curation. **Yi Xiaoping:** Writing – review & editing, Methodology, Funding acquisition, Data curation. **Huang Deyou:** Methodology, Data curation. **Mao Yipu:** Methodology, Data curation.

Declaration of Competing Interest

The authors declare no competing interests.

Acknowledgments

We thank staff members in the Departments of Radiology,

Neurosurgery, and Pathology at all participating Hospitals for their efforts in collecting the information used in this study, and for their helpful discussion and assistance in the data analysis and manuscript preparation. We thank Drs. Guanghui Gong, Qingling Li, Hongling Yin, Jingjing Zeng, Juan He, and Yiwu Dang from the Department of Pathology at Xiangya Hospital, Central South University and First Affiliated Hospital of Guangxi Medical University for assistance in the pathological analysis. We thank Xiangrong Li, Yuhong Qin, and Liling Long, from First Affiliated Hospital of Guangxi Medical University for their helpful suggestions for collecting the information.

Data Availability

The data for this study can be shared on reasonable request to the corresponding author.

References

[1] A. Lester, K.L. McDonald, Intracranial ependymomas: molecular insights and translation to treatment, Brain Pathol. 30 (1) (2020) 3–12.
[2] E.L. Yuh, A.J. Barkovich, N. Gupta, Imaging of ependymomas: MRI and CT, Childs Nerv. Syst. 25 (10) (2009) 1203–1213.
[3] T. Larrew, et al., Molecular Classification and Therapeutic Targets in Ependymoma, Cancers (Basel) 13 (24) (2021).
[4] R. Ruda, et al., Ependymoma: Evaluation and Management Updates, Curr. Oncol. Rep. 24 (8) (2022) 985–993.
[5] D.N. Louis, et al., The 2021 WHO Classification of Tumors of the Central Nervous System: a summary, Neuro Oncol. 23 (8) (2021) 1231–1251.
[6] N.K. Foreman, et al., Second-look surgery for incompletely resected fourth ventricle ependymomas: technical case report, Neurosurgery 40 (4) (1997) 856–860, discussion 860.
[7] E. Bouffet, et al., Intracranial ependymomas in children: a critical review of prognostic factors and a plea for cooperation, Med Pedia Oncol. 30 (6) (1998) 319–329, discussion 329-31.
[8] K.P. Haresh, et al., Prognostic Factors and Survival Outcomes of Intracranial Ependymoma Treated with Multimodality Approach, Indian J. Med Paediatr. Oncol. 38 (4) (2017) 420–426.
[9] A. Jenseit, et al., EZHIP: a new piece of the puzzle towards understanding pediatric posterior fossa ependymoma, Acta Neuropathol. 143 (1) (2022) 1–13.
[10] T.E. Merchant, et al., Conformal radiotherapy after surgery for paediatric ependymoma: a prospective study, Lancet Oncol. 10 (3) (2009) 258–266.
[11] B. Timmermann, et al., Role of radiotherapy in anaplastic ependymoma in children under age of 3 years: results of the prospective German brain tumor trials HIT-SKK 87 and 92, Radio. Oncol. 77 (3) (2005) 278–285.
[12] M. Reni, et al., A multicenter study of the prognosis and treatment of adult brain ependymal tumors, Cancer 100 (6) (2004) 1221–1229.
[13] Y.H. Chai, et al., Ependymomas: Prognostic Factors and Outcome Analysis in a Retrospective Series of 33 Patients, Brain Tumor Res Treat. 5 (2) (2017) 70–76.
[14] J.K. Park, et al., Scale to predict survival after surgery for recurrent glioblastoma multiforme, J. Clin. Oncol. 28 (24) (2010) 3838–3843.
[15] Z. Jia, et al., Development and validation of prognostic nomogram in ependymoma: A retrospective analysis of the SEER database, Cancer Med 10 (17) (2021) 6140–6148.
[16] T. Hollon, et al., Supratentorial hemispheric ependymomas: an analysis of 109 adults for survival and prognostic factors, J. Neurosurg. 125 (2) (2016) 410–418.
[17] Y. Zhang, et al., Bladder cancer survival nomogram: Development and validation of a prediction tool, using the SEER and TCGA databases, Med. (Baltim.) 98 (44) (2019) e17725.
[18] X. Wang, et al., Development and Validation of a Prognostic Nomogram in AFP-negative hepatocellular carcinoma, Int J. Biol. Sci. 15 (1) (2019) 221–228.
[19] C. Fakhry, et al., Development and Validation of Nomograms Predictive of Overall and Progression-Free Survival in Patients With Oropharyngeal Cancer, J. Clin. Oncol. 35 (36) (2017) 4057–4065.
[20] L. Huang, et al., Development and validation of a prognostic model to predict the prognosis of patients who underwent chemotherapy and resection of pancreatic adenocarcinoma: a large international population-based cohort study, BMC Med 17 (1) (2019) 66.
[21] J. Cao, et al., Clinical Nomogram for Predicting Survival of Esophageal Cancer Patients after Esophagectomy, Sci. Rep. 6 (2016) 26684.
[22] J.C. Peeken, et al., Combining multimodal imaging and treatment features improves machine learning-based prognostic assessment in patients with glioblastoma multiforme, Cancer Med 8 (1) (2019) 128–136.
[23] M. Nicolasjilwan, et al., Addition of MR imaging features and genetic biomarkers strengthens glioblastoma survival prediction in TCGA patients, J. Neuroradiol. 42 (4) (2015) 212–221.
[24] R. Jain, et al., Outcome prediction in patients with glioblastoma by using imaging, clinical, and genomic biomarkers: focus on the nonenhancing component of the tumor, Radiology 272 (2) (2014) 484–493.
[25] J.C. Peeken, et al., Semantic imaging features predict disease progression and survival in glioblastoma multiforme patients, Strahl. Onkol. 194 (6) (2018) 580–590.
[26] A. Rao, et al., A combinatorial radiographic phenotype may stratify patient survival and be associated with invasion and proliferation characteristics in glioblastoma, J. Neurosurg. 124 (4) (2016) 1008–1017.
[27] P.C. Austin, Graphical methods to illustrate the nature of the relation between a continuous variable and the outcome when using restricted cubic splines with a Cox proportional hazards model, Stat. Methods Med Res 34 (2) (2025) 277–285.
[28] N. Sun, et al., A novel 14-gene signature for overall survival in lung adenocarcinoma based on the Bayesian hierarchical Cox proportional hazards model, Sci. Rep. 12 (1) (2022) 27.
[29] G.S. Collins, et al., Transparent reporting of a multivariable prediction model for individual prognosis or diagnosis (TRIPOD): the TRIPOD statement, BMJ 350 (2015) g7594.
[30] Y. Yao, et al., Nomogram incorporating preoperative MRI-VASARI features for differentiating intracranial extraventricular ependymoma from glioblastoma, Quant. Imaging Med Surg. 14 (3) (2024) 2255–2266.
[31] D. She, et al., MR Imaging Features of Anaplastic Pleomorphic Xanthoastrocytoma Mimicking High-Grade Astrocytoma, AJNR Am. J. Neuroradiol. 39 (8) (2018) 1446–1452.
[32] Z. Xing, et al., Noninvasive Assessment of IDH Mutational Status in World Health Organization Grade II and III Astrocytomas Using DWI and DSC-PWI Combined with Conventional MR Imaging, AJNR Am. J. Neuroradiol. 38 (6) (2017) 1138–1144.
[33] Z. Xing, et al., IDH genotypes differentiation in glioblastomas using DWI and DSC-PWI in the enhancing and peri-enhancing region, Acta Radio. 60 (12) (2019) 1663–1672.
[34] P. Wangaryattawanich, et al., Multicenter imaging outcomes study of The Cancer Genome Atlas glioblastoma patient cohort: imaging predictors of overall and progression-free survival, Neuro Oncol. 17 (11) (2015) 1525–1537.
[35] M. Park, et al., Elderly patients with newly diagnosed glioblastoma: can preoperative imaging descriptors improve the predictive power of a survival model? J. Neurooncol 134 (2) (2017) 423–431.
[36] M.A. Mazurowski, A. Desjardins, J.M. Malof, Imaging descriptors improve the predictive power of survival models for glioblastoma patients, Neuro Oncol. 15 (10) (2013) 1389–1394.
[37] D. Spagnoli, et al., Combined treatment of fourth ventricle ependymomas: report of 26 cases, Surg. Neurol. 54 (1) (2000) 19–26, discussion 26.
[38] H. Zhou, et al., MRI features predict survival and molecular markers in diffuse lower-grade gliomas, Neuro Oncol. 19 (6) (2017) 862–870.